

# Spectra of "Real-World" Graphs: Beyond the Semi-Circle Law

Illes J. Farkas<sup>1</sup>, Imre Derenyi<sup>2,3</sup>, Albert-Laszlo Barabasi<sup>2,4</sup>, Tamás Vicsek<sup>1,2</sup>

<sup>1</sup> Department of Biological Physics, Eotvos University, Budapest, Pazmany Peter Setany 1A, H-1117 Hungary

<sup>2</sup> Collegium Budapest, Institute for Advanced Study, Budapest, Szentharomsag utca 2, H-1014 Hungary

<sup>3</sup> Institut Curie, UMR 168, 26 rue d'Ulm, F-75248 Paris 05, France

<sup>4</sup> Department of Physics, University of Notre Dame, Notre Dame, IN 46556  
fij@elte.hu, derenyi@angel.elte.hu, alb@nd.edu, vicsek@angel.elte.hu

Many natural and social systems develop complex networks, that are usually modelled as random graphs. The eigenvalue spectrum of these graphs provides information about their structural properties. While the semi-circle law is known to describe the spectra of uncorrelated random graphs, much less is known about the spectra of real-world graphs, describing such complex systems as the Internet, metabolic pathways, networks of power stations, scientific collaborations or movie actors, which are inherently correlated and usually very sparse. An important limitation in addressing the spectra of these systems is that the numerical determination of the spectra for systems with more than a few thousand nodes is prohibitively time and memory consuming. Making use of recent advances in algorithms for spectral characterization, here we develop new methods to determine the eigenvalues of networks comparable in size to real systems, obtaining several surprising results on the spectra of adjacency matrices corresponding to models of real-world graphs. We find that when the number of links grows as the number of nodes, the spectrum of uncorrelated random matrices does not converge to the semi-circle law. Furthermore, the spectra of real-world graphs have specific features depending on the details of the corresponding models. In particular, scale-free graphs develop a triangle-like spectrum with a power law tail, while small-world graphs have a complex spectrum consisting of several sharp peaks. These and further results indicate that the spectra of correlated graphs represent a practical tool for graph classification and can provide useful insight into the relevant structural properties of real networks.

## I. INTRODUCTION

Random graphs [1,2] have long been used for modelling the evolution and topology of systems made up of large assemblies of similar units. The uncorrelated random graph model which assumes each pair of the graph's vertices to be connected with equal and independent probabilities treats a network as an assembly of equivalent units. This model, introduced by the mathematicians Paul Erdős and Alfred Rényi [1], has been much investigated in the mathematical literature [2]. However, the increasing availability of large maps of real-life networks has indicated that real networks are fundamentally correlated systems, and in many respects their topology deviates from the uncorrelated random graph model. Consequently, the attention has shifted towards more advanced graph models which are designed to generate topologies in line with the existing empirical results [3-14]. Examples of real networks, that serve as a benchmark for the current modelling efforts include the Internet [6,15-17], the World-Wide Web [8,18], networks of collaborating movie actors and those of collaborating scientists [13,14], the power grid [4,5] and the metabolic network of numerous living organisms [9,19].

These are the systems that we will call "real-world" networks or graphs. Several converging reasons explain the enhanced current interest in such real graphs. First, the amount of topological data available on such large structures has increased dramatically during the past few years thanks to the computerization of data collection

in various fields, from sociology to biology. Second, the hitherto unseen speed of growth of some of these complex networks (e.g., the Internet) and their pervasiveness in affecting many aspects of our life has created the need to understand the topology, origin and evolution of such structures. Finally, the increased computational power available on almost every desktop has allowed, for the first time, to study such systems in unprecedented detail.

The proliferation of data has led to a flurry of activity towards understanding the general properties of real networks. These efforts have resulted in the introduction of two classes of models, commonly called small-world graphs [4,5] and the scale-free networks [10,11]. The first aims to capture the clustering observed in real graphs, while the second reproduces the power law degree distribution present in many real networks. However, until now, most analyses of these models and data sets have been confined to real-space characteristics, that capture their static structural properties: e.g., degree sequences, shortest connecting paths and clustering coefficients. In contrast, there is extensive literature demonstrating that the properties of graphs and the associated adjacency matrices are well characterized by spectral methods, that provide global measures of the network properties [20,21]. In this paper, we offer a detailed analysis of the most studied network models using algebraic tools intrinsic to large random graphs.

The paper is organized as follows. Section II introduces the main random graph models used for the topological

description of large assemblies of connected units. Section III lists the { analytical and numerical } tools which we used and developed to convert the topological features of graphs into algebraic invariants. Section IV contains our results concerning the spectra and special eigenvalues of the three main types of random graph models: sparse uncorrelated random graphs in Section IV A; small-world graphs in Section IV B; and scale-free networks in Section IV C. Section IV D gives simple algorithms for testing the graph's structure, and Section IV E investigates the variance of structure within single random graph models.

## II. MODELS OF RANDOM GRAPHS

### A. The uncorrelated random graph model and the semi-circle law

#### 1. Definitions

Throughout this paper, we will use the term "graph" for a set of points (vertices) connected by undirected lines (edges); no multiple edges and no loops connecting a vertex to itself are allowed. We will call two vertices of the graph "neighbors", if they are connected by an edge. Based on Ref. [1], we shall use the term "uncorrelated random graph" for a graph, if (i) the probability for any pair of the graph's vertices being connected is the same,  $p$ ; (ii) these probabilities are independent variables.

Any graph  $G$  can be represented by its adjacency matrix,  $A(G)$ , which is a real symmetric matrix:  $A_{ij} = A_{ji} = 1$ , if vertices  $i$  and  $j$  are connected, or 0, if these two vertices are not connected. The main algebraic tool which we will use for the analysis of graphs will be the spectrum { i.e., the set of eigenvalues } of the graph's adjacency matrix. The spectrum of the graph's adjacency matrix is also called the spectrum of the graph.

#### 2. Applying the semi-circle law for the spectrum of the uncorrelated random graph

A general form of the semi-circle law for real symmetric matrices is the following [20,22,23]. If  $A$  is a real symmetric  $N \times N$  uncorrelated random matrix,  $\langle A_{ij} \rangle = 0$  and  $\langle A_{ij}^2 \rangle = p$  for every  $i \neq j$ , and with increasing  $N$  each moment of each  $A_{ij}$  remains finite, then in the  $N \rightarrow \infty$  limit the spectral density { i.e., the density of eigenvalues } of  $A = N^{-1} \sum_{i,j} A_{ij} e^{i\lambda_j}$  converges to the semi-circular distribution:

$$\rho(\lambda) = \begin{cases} \frac{2}{\pi} \sqrt{4 - \lambda^2} & \text{if } |\lambda| \leq 2 \\ 0 & \text{otherwise.} \end{cases} \quad (1)$$

This theorem is also known as Wigner's law [22], and its extensions to further matrix ensembles have long been used for the stochastic treatment of complex quantum

mechanical systems lying far beyond the reach of exact methods [24,25]. Later, the semi-circle law was found to have many applications in statistical physics and solid-state physics as well [20,21,26].

Note, that for the adjacency matrix of the uncorrelated random graph many of the semi-circle law's conditions do not hold, e.g., the expectation value of the entries is a non-zero constant:  $p \neq 0$ . Nevertheless, in the  $N \rightarrow \infty$  limit, the rescaled spectral density of the uncorrelated random graph converges to the semi-circle law of Eq. (1) [27]. An illustration of the convergence of the average spectral density to the semi-circular distribution can be seen on Fig.1. It is necessary to make a comment concerning figures here. In order to keep figures simple, for the spectral density plots we have chosen to show the spectral density of the original matrix,  $A$ , and to rescale the horizontal ( $\lambda$ ) and vertical ( $\rho$ ) axes by  $\lambda \rightarrow \lambda \sqrt{N p(1-p)}$  and  $\rho \rightarrow \rho \sqrt{N p(1-p)}$ .

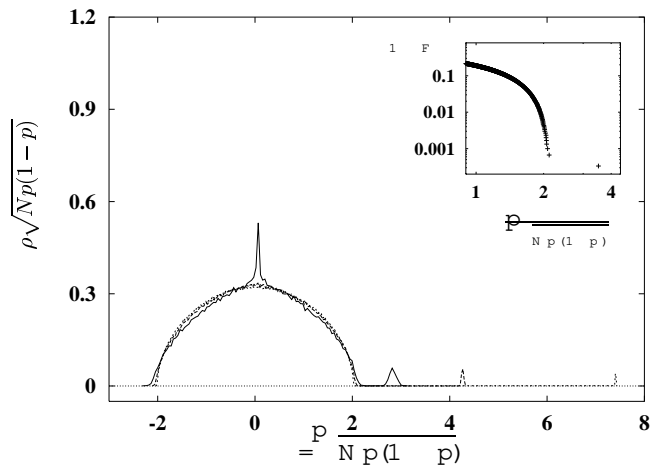


FIG. 1. If  $N \rightarrow \infty$  and  $p = \text{const}$ , the average spectral density of an uncorrelated random graph converges to a semi-circle, the first eigenvalue grows as  $\sqrt{N}$ , and the second is proportional to  $\sqrt{N}$  (see Section IIA). Main panel: The spectral density is shown for  $p = 0.05$  and three different system sizes:  $N = 100$  (|),  $N = 300$  ({} ) and  $N = 1000$  (---). In all three cases, the complete spectrum of 1000 graphs was computed and averaged. Inset: At the edge of the semi-circle { i.e., in the  $\lambda \approx 2 \sqrt{N p(1-p)}$  regions, } the spectral density decays exponentially, and with  $N \rightarrow \infty$ , the decay rate diverges [20,29]. Here,  $F(\lambda) = N^{-1} \sum_{i < j} 1$  is the cumulative spectral distribution function, and  $\lambda \approx 2 \sqrt{N p(1-p)}$  is shown for a graph with  $N = 3;000$  vertices and 15;000 edges.

Some further results on the behavior of the uncorrelated random graph's eigenvalues, relevant for the analysis of real-world graphs as well, include the following: The principal eigenvalue (the largest eigenvalue,  $\lambda_1$ ) grows much faster than the second eigenvalue:  $\lim_{N \rightarrow \infty} (\lambda_1 - N) = p$  with probability 1, whereas for every  $\lambda > 1=2$ ,  $\lim_{N \rightarrow \infty} (\lambda_2 - N) = 0$ . (see Refs. [27,28] and Fig.1.). A similar relation holds for the smallest eigen-

value,  $\langle k \rangle$ : for every  $k > 1=2$ ,  $\lim_{N \rightarrow \infty} \frac{1}{N} \sum_{i=1}^N k_i = \langle k \rangle$ . In other words: if  $k_i$  denotes the average number of connections of a vertex in the graph, then  $\langle k \rangle$  scales as  $\langle k \rangle \sim N^{-1}$ , and the width of the "bulk" part of the spectrum { the set of the eigenvalues  $\lambda_i$ ;  $i=1, \dots, N$  } scales as  $\sim N^{-1/2}$ . Lastly, the semi-circular distribution's edges are known to decay exponentially, and the number of eigenvalues in the  $\lambda > 0$  ( $N$ ) tail has been shown to be of the order of 1 [20,29].

## B. Real-world graphs

The two main models proposed to describe real-world graphs are the small-world model and the scale-free model.

### 1. Small-world graphs

The small-world graph [4,5,30] is created by randomly rewiring some of the edges of a regular [31] ring graph. The regular ring graph is created as follows. First draw the vertices  $1, 2, \dots, N$  on a circle in ascending order. Then, for every  $i$ , connect vertex  $i$  to the vertices lying closest to it on the circle: vertices  $i-k, \dots, i-1, i+1, \dots, i+k$ , where every number should be understood modulo  $N$  ( $k$  is an even number). Fig. 9 shows, that this algorithm creates a regular graph indeed, because the degree [31] of any vertex is the same number,  $k$ . Next, starting from vertex 1 and proceeding towards  $N$ , perform the rewiring step. For vertex 1, consider the "first forward connection", i.e., the connection to vertex 2. With probability  $p_r$ , reconnect vertex 1 to another vertex chosen uniformly at random and without allowing multiple edges. Proceed towards the remaining forward connections of vertex 1, and then, perform this step for the remaining  $N-1$  vertices also. For the rewiring, use equal and independent probabilities. Note, that in the small-world model the density of edges is  $p = \langle k \rangle / (N-1)$  ( $k=N$ ). Throughout this paper, we will use only  $k > 2$ .

If we use  $p_r = 0$  in the small-world model, the original regular graph is preserved, and for  $p_r = 1$ , one obtains a random graph which differs from the uncorrelated random graph only slightly: every vertex has a minimum degree of  $k=2$ . Next, we will need two definitions. The separation between vertices  $i$  and  $j$  { denoted by  $L_{ij}$  } is the number of edges in the shortest path connecting them. The clustering coefficient at vertex  $i$  { denoted by  $C_i$  } is the number of existing edges among the neighbors of vertex  $i$  divided by the number of all possible connections between them. In the small-world model, both  $L_{ij}$  and  $C_i$  are functions of the rewiring probability,  $p_r$ . Based on the above definitions of  $L_{ij}(p_r)$  and  $C_i(p_r)$ , the characteristics of the small-world phenomenon { which occurs for intermediate values of  $p_r$  } can be given as follows [4,5]: (i) the average separation between two vertices,  $L(p_r)$ ,

drops dramatically below  $L(p_r = 0)$ , whereas (ii) the average clustering coefficient,  $C(p_r)$ , remains high, close to  $C(p_r = 0)$ . Note, that the rewiring procedure is carried out independently for every edge, therefore the degree sequence and also other distributions in the system { e.g., path length and loop size } decay exponentially.

### 2. The scale-free model

The scale-free model assumes a random graph to be a growing set of vertices and edges, where the location of new edges is determined by a preferential attachment rule [10,11]. Starting from an initial set of  $m_0$  isolated vertices, one adds 1 new vertex and  $m$  new edges at every time step  $t$ . (Throughout this paper, we will use  $m = m_0$ .) The  $m$  new edges connect the new vertex and  $m$  different vertices chosen from the  $N$  old vertices. The  $i$ th old vertex is chosen with probability  $k_i / \sum_{j=1}^N k_j$ , where  $k_i$  is the degree of vertex  $i$ . (The density of edges in a scale-free graph is  $p = \langle k \rangle / (N-1)$  ( $2m=N$ .) In contrast to the small-world model, the distribution of degrees in a scale-free graph converges to a power-law when  $N \rightarrow \infty$ , which has been shown to be a combined effect of growth and the preferential attachment [11]. Thus, in the infinite time or size limit, the scale-free model has no characteristic scale in the degree size [4,32,37].

### 3. Related models

Lately, numerous other models have been suggested for a unified description of real-world graphs [4,32,35,37,40]. Models of growing networks with aging vertices were found to display both heavy tailed and exponentially decaying degree sequences [34,36] as a function of the speed of aging. Generalized preferential attachment rules have helped us better understand the origin of the exponents and correlations emerging in these systems [32,33]. Also, investigations of more complex network models { using aging or an additional fixed cost of edges [2] or preferential growth and random rewiring [37] } have shown, that in the "frequent rewiring, fast aging, high cost" limiting case, one obtains a graph with an exponentially decaying degree sequence, whereas in the "no rewiring, no aging, zero cost" limiting case the degree sequence will decay as a power-law. According to studies of scientific collaboration networks [13,14] and further social and biological structures [2,19,41], a significant proportion of large networks lies between the two extremes. In such cases, the characterization of the system using a small number of algebraic constants could facilitate the classification of real-world networks.

### III. TOOLS

#### A. Analytical

##### 1. The spectrum of the graph

The spectrum of a graph is the set of eigenvalues of the graph's adjacency matrix. The physical meaning of a graph's eigenpair (an eigenvector and its eigenvalue) can be illustrated by the following example. Write each component of a vector  $\mathbf{v}$  on the corresponding vertex of the graph:  $v_i$  on vertex  $i$ . Next, on every vertex write the sum of the numbers found on the neighbors of vertex  $i$ . If the resulting vector is a multiple of  $\mathbf{v}$ , then  $\mathbf{v}$  is an eigenvector, and the multiplier is the corresponding eigenvalue of the graph.

The spectral density of a graph is the density of the eigenvalues of its adjacency matrix. For a finite system, this can be written as a sum of delta functions

$$D(\lambda) = \frac{1}{N} \sum_{j=1}^N \delta(\lambda - \lambda_j); \quad (2)$$

which converges to a continuous function with  $N \rightarrow \infty$  ( $\lambda_j$  is the  $j$ th largest eigenvalue of the graph's adjacency matrix).

The spectral density of a graph can be directly related to the graph's topological features: the  $k$ th moment,  $M_k$ , of  $D(\lambda)$  can be written as

$$\begin{aligned} M_k &= \frac{1}{N} \sum_{j=1}^N (\lambda_j)^k = \frac{1}{N} \text{Tr} A^k = \\ &= \frac{1}{N} \sum_{i_1, i_2, \dots, i_k} A_{i_1 i_2} A_{i_2 i_3} \dots A_{i_k i_1} \end{aligned} \quad (3)$$

From the topological point of view,  $D_k = N M_k$  is the number of directed paths (loops) of the underlying (undirected) graph, that return to their starting vertex after  $k$  steps. On a tree, the length of any such path can be an even number only, because these paths contain any edge an even number of times: once such a path has left its starting point by choosing a starting edge, no alternative route for returning to the starting point is available. However, if the graph contains loops of odd length, the path length can be an odd number, as well.

##### 2. Extreme eigenvalues

In an uncorrelated random graph the principal eigenvalue,  $\lambda_1$ , shows the density of edges and  $\lambda_2$  can be related to the conductance of the graph as a network of resistances [42]. An important property of all graphs is the following: the principal eigenvector,  $\mathbf{e}_1$ , of the adjacency matrix is a non-negative vector (all components

are non-negative), and if the graph has no isolated vertices,  $\mathbf{e}_1$  is a positive vector [43]. All other eigenvectors are orthogonal to  $\mathbf{e}_1$ , therefore they all have entries with mixed signs.

##### 3. The inverse participation ratios of eigenvectors

The inverse participation ratio of the normalized  $j$ th eigenvector,  $\mathbf{e}_j$ , is defined as [26]

$$I_j = \sum_{k=1}^N (e_j)_k^4; \quad (4)$$

If the components of an eigenvector are identical ( $(e_j)_i = 1/\sqrt{N}$  for every  $i$ ), then  $I_j = 1/N$ . For an eigenvector with one single non-zero component ( $(e_j)_i = \delta_{ij}$ ) the inverse participation ratio is 1. The comparison of these two extreme cases illustrates that with the help of the inverse participation ratio, one can tell whether only  $O(1)$  or as many as  $O(N)$  components of an eigenvector differ significantly from 0, i.e., whether an eigenvector is localized or non-localized.

#### B. Numerical

##### 1. General real symmetric eigenvalue solver

To compute the eigenpairs of graphs below the size  $N = 5,000$ , we used the general real symmetric eigenvalue solver of Ref. [44]. This algorithm requires the allocation of memory space to all entries of the matrix, thus to compute the spectrum of a graph of size  $N = 20,000$  ( $N = 1,000,000$ ) using this general method with double precision floating point arithmetic, one would need 32 GB (8 TB) memory space and the execution of approximately  $30 N^2 = 1.2 \cdot 10^{10}$  ( $3 \cdot 10^{13}$ ) floating point operations [44]. Consequently, we need to develop more efficient algorithms to investigate the properties of graphs with sizes comparable to real-world networks.

##### 2. Iterative eigenvalue solver based on the thick-restart Lanczos algorithm

The spectrum of a real-world graph is the spectrum of a sparse real symmetric matrix, therefore the most efficient algorithms which can give a handful of the top  $n_d$  eigenvalues (and the corresponding eigenvectors) of a large graph are iterative methods [45]. These methods allow the matrix to be stored in any compact format, as long as matrix-vector multiplication can be carried out at a high speed. Iterative methods use little memory: only the non-zero entries of the matrix and a few vectors of size  $N$  need to be stored. The price for computational speed lies in the number of the obtained eigenvalues: iterative methods compute only a handful of the largest

(or smallest) eigenvalues of a matrix. To compute the eigenvalues of graphs above the size  $N = 5,000$ , we have developed algorithms using a specially modified version of the thick-restart Lanczos algorithm [46,47]. The modifications and some of the main technical parameters of our software are explained in the following paragraphs.

Even though iterative eigenvalue methods are mostly used to obtain the top eigenvalues of a matrix, after minor modifications the internal eigenvalues in the vicinity of a fixed  $\lambda_0$  point can be computed as well. For this, extremely sparse matrices are usually "shift-inverted", i.e., to find those eigenvalues of  $A$  that are closest to  $\lambda_0$ , the highest and lowest eigenvalues of  $(A - \lambda_0 I)^{-1}$  are searched for. However, because of the extremely high cost of matrix inversion in our case, for the computation of internal eigenvalues we suggest to use the "shift-square" method with the matrix

$$B = \lambda_0^{-2} (A - \lambda_0 I)^{2n+1} \quad (5)$$

Here  $\lambda_0$  is the largest eigenvalue of  $(A - \lambda_0 I)^2$ ,  $I$  is the identity matrix and  $n$  is a positive integer. Transforming the matrix  $A$  into  $B$  transforms the spectrum of  $A$  in the following manner. First, the spectrum is shifted to the left by  $\lambda_0$ . Then, the spectrum is "folded" (and squared) at the origin such that all eigenvalues will be negative. Next, the spectrum is linearly rescaled and shifted to the right, with the following effect: (i) the whole spectrum will lie in the symmetric interval  $[-2; 2]$  and (ii) those eigenvalues that were closest to  $\lambda_0$  in the spectrum of  $A$ , will be the largest now, i.e., they will be the eigenvalues closest to  $-2$ . Now, raising all eigenvalues to the  $(2n+1)$ st power increases the relative difference,  $1 - \lambda_i/\lambda_j$ , between the top eigenvalues  $\lambda_i$  and  $\lambda_j$  by a factor of  $2n+1$ . This allows the iterative method find the top eigenvalues of  $B$  more quickly. One can compute the corresponding eigenvalues (those being closest to  $\lambda_0$ ) of the original matrix,  $A$ : if  $\tilde{v}_1, \tilde{v}_2, \dots, \tilde{v}_{n_d}$  are the normalized eigenvectors of the  $n_d$  largest eigenvalues of  $B$ , then for  $A$  the  $n_d$  eigenvalues closest to  $\lambda_0$  will be  $\{\lambda_1, \lambda_2, \dots, \lambda_{n_d}\}$  not necessarily in ascending order  $\{\tilde{v}_1 A \tilde{v}_1, \tilde{v}_2 A \tilde{v}_2, \dots, \tilde{v}_{n_d} A \tilde{v}_{n_d}\}$ .

The thick-restart Lanczos method uses memory space for the non-zero entries of the  $N \times N$  large adjacency matrix, and  $n_g + 1$  vectors of length  $N$ , where  $n_g$  ( $n_g > n_d$ ) is usually between 10 and 100. Besides the relatively small size of required memory, we could also exploit the fact that the non-zero entries of a graph's adjacency matrix are all 1's: during matrix-vector multiplication (which is usually the most time-consuming step of an iterative method) only additions had to be carried out instead of multiplications.

The numerical spectral density functions of large graphs ( $N = 5,000$ ) of this paper were obtained using the following steps. To compute the spectral density of the adjacency matrix,  $A$ , at an internal  $\lambda_0$  location, first, the  $n_d$  eigenvalues closest to  $\lambda_0$  were searched for. Next, the distance between the smallest and the largest

of the obtained eigenvalues was computed. Finally,  $(\lambda_0 - \lambda_{\min})$  this distance was multiplied by  $N = (n_d - 1)$ , and was averaged using  $n_{av}$  different graphs. We used double precision floating point arithmetic, and the iterations were stopped, if (i) at least  $n_{it}$  iterations had been carried out and (ii) the lengths of the residual vectors belonging to the  $n_d$  selected eigenpairs were all below  $\epsilon = 10^{-12}$  [46].

## IV. RESULTS

### A. Sparse uncorrelated random graphs: the semi-circle law is not universal

In the uncorrelated random graph model of Erdős and Renyi, the total number of edges grows quadratically with the number of vertices:  $N_{edge} = N \langle k_i \rangle = N p(N-1) \approx pN^2$ . However, in many real-world graphs edges are "expensive", and the growth rate of the number of connections remains well below this rate. For this reason, we also investigated the spectra of such uncorrelated networks, for which the probability of any two vertices being connected changes with the size of the system using  $pN = c = \text{const.}$  Two special cases are  $c = 0$  (the Erdős-Renyi model) and  $c = 1$ . In the second case,  $pN \rightarrow \text{const.}$  as  $N \rightarrow \infty$ , i.e., the average degree remains constant.

For  $c < 1$  and  $N \rightarrow \infty$ , there exists an infinite cluster of connected vertices (in fact, it exists for every  $c > 0$ ). Moreover, the expectation value of any  $k_i$  converges to infinity, thus any vertex is almost surely connected to the infinite cluster. The spectral density function converges to the semicircular distribution of Eq. (1), because the total weight of isolated subgraphs decreases exponentially with growing system size. (A detailed analysis of this issue is available in Ref. [48].)

For  $c = 1$  and  $N \rightarrow \infty$  (see Fig. 2), the probability for a vertex to belong to a cluster of any finite size remains also finite [49]. Therefore, the limiting spectral density contains the weighted sum of the spectral densities of all finite graphs [50]. The most striking deviation from the semi-circle law in this case is the elevated central part of the spectral density. The probability for a vertex to belong to an isolated cluster of size  $s$  decreases exponentially with  $s$  [49], therefore the number of large isolated clusters is low and the eigenvalues of a graph with  $s$  vertices are bounded by  $\sqrt{s-1}$  and  $-\sqrt{s-1}$ . For these two reasons, the amplitudes of delta functions decay exponentially, as the absolute value of their locations,  $|j|$ , increases.

The principal eigenvalue of this graph converges to a constant:  $\lim_{N \rightarrow \infty} (\lambda_1) = pN = c$ , and  $(\lambda_1)$  will be symmetric in the  $N \rightarrow \infty$  limit. Therefore, in the limit, all odd moments ( $M_{2k+1}$ ), and thus, the number of all loops with odd length ( $D_{2k+1}$ ) disappear. This is a salient feature of graphs with tree structure (because on a tree every edge must be used an even number of times in order to

return to the initial vertex), indicating that the structure of a sparse uncorrelated random graph becomes more and more tree-like. This can also be understood by considering that the typical distance (length of the shortest path) between two vertices on both a sparse uncorrelated random graph and a regular tree with the same number of edges scales as  $\ln(N)$ . So except for a few short-cuts a sparse uncorrelated random graph looks like a tree.

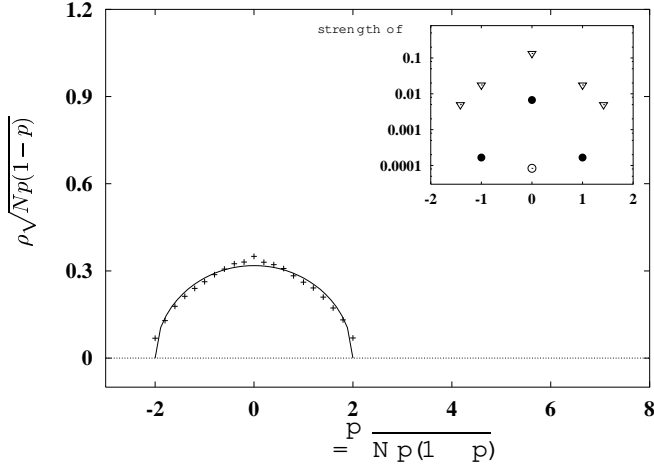


FIG. 2. If  $N \gg 1$  and  $pN = \text{const}$ , the spectral density of the uncorrelated random graph does not converge to a semi-circle. Main panel: Symbols show the spectrum of an uncorrelated random graph (20;000 vertices and 100;000 edges) measured with the iterative method using  $n_{av} = 1$ ,  $n_d = 101$  and  $n_g = 250$ . A solid line shows the semi-circular distribution for comparison. (Note, that the principal eigenvalue,  $\lambda_1$ , is not shown here, because here at any  $\lambda = 0$  point the average first neighbor distance among  $n_d = 101$  eigenvalues was used to measure the spectral density.) Inset: Strength of delta functions in  $\rho(\lambda)$  "caused" by isolated clusters of sizes 1, 2 and 3 in uncorrelated random graphs (see Ref. [50] for a detailed explanation). Symbols are for graphs with 20;000 vertices and 20;000 edges ( $\nabla$ ), 50;000 edges ( $\square$ ), and 100;000 edges ( $\circ$ ). Results were averaged for 3 different graphs everywhere.

## B. The small-world graph

### 1. Triangles are abundant in the graph

For  $p_r = 0$ , the small-world graph is regular and also periodical. Because of the highly ordered structure,  $\rho(\lambda)$  contains numerous singularities, which are listed in Section VIA (see also Fig. 3). Note that  $\rho(\lambda)$  has a high third moment. (Remember, that we use only  $k > 2$ .)

If we increase  $p_r$  such that the small-world region is reached, i.e., the periodical structure of the graph is perturbed, then singularities become blurred and are transformed into high local maxima, but  $\rho(\lambda)$  retains a strong skewness (see Fig. 3). This is in good agreement with

results of Refs. [30,51], where it has been shown that the local structure of the small-world graph is ordered, however, already a very small number of shortcuts can drastically change the graph's global structure.

In the  $p_r = 1$  case the small-world model becomes very similar to the uncorrelated random graph: the only difference is that here, the minimum degree of any vertex is a positive constant,  $k=2$ , whereas in an uncorrelated random graph the degree of a vertex can be any non-negative number. Accordingly,  $\rho(\lambda)$  becomes a semi-circle for  $p_r = 1$  (Fig. 3). Nevertheless, it should be noted, that as  $p_r$  converges to 1, a high value of  $M_3$  is preserved even for  $p_r$  close to 1, where all local maxima have already vanished. The third moment of  $\rho(\lambda)$  gives the number of triangles in the graph (see Section III A 1); the lack of high local maxima (i.e., the remnants of singularities) shows the absence of an ordered structure. From the above we conclude, that from the spectrum's point of view the high number of triangles is one of the most basic properties of the small-world model, and it is preserved much longer, than regularity or periodicity, if the level of randomness,  $p_r$ , is increased.

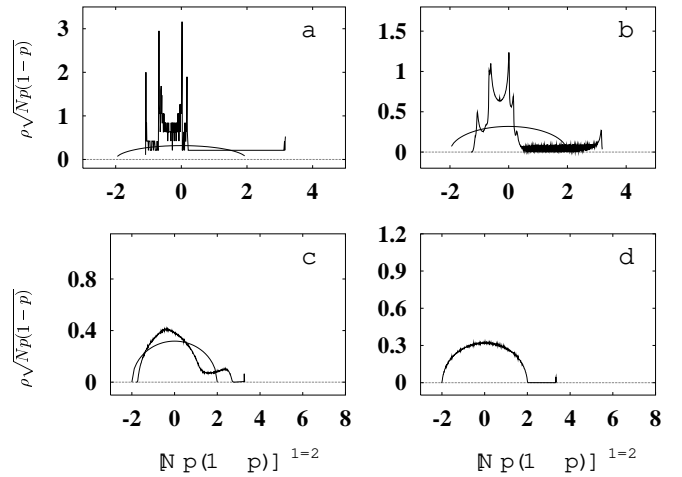


FIG. 3. Spectral densities of small-world graphs using the complete spectra. The solid line shows the semi-circular distribution for comparison. (a) Spectral density of the regular ring graph created from the small-world model with  $p_r = 0$ ,  $k = 10$  and  $N = 1000$ . (b) For  $p_r = 0.01$ , the average spectral density of small-world graphs contains sharp maxima, which are the "blurred" remnants of the singularities of the  $p_r = 0$  case. Topologically, this means, that the graph is still almost regular, but it contains a small number of impurities. In other words, after a small perturbation, the system is no more degenerate. (c) The average spectral density computed for the  $p_r = 0.3$  case shows that the third moment of  $\rho(\lambda)$  is preserved even for very high values of  $p_r$ , where there is already no sign of any blurred singularity (i.e., regular structure). This means, that even though all remaining regular islands have been destroyed already, triangles are still dominant. (d) If  $p_r = 1$ , then the spectral density of the small-world graph converges to a semi-circle. In figures b, c and d, 1000 different graphs with  $N = 1000$  and  $k = 10$  were used for averaging.

For  $m = m_0 = 1$ , the scale-free graph is a tree by definition and its spectrum is symmetric [43]. In the  $m > 1$  case ( ) consists of several well distinguishable parts (see Fig.4). The "bulk" part of the spectral density { the set of the eigenvalues  $f_{2; \dots; N} g$  } converges to a symmetric continuous function which has a triangle-like shape for the normalized values up to 1.5 and has power-law tails.

The central part of the spectral density converges to a triangle-like shape with its top lying well above the semi-circle. Since the scale-free graph is fully connected by definition, the increased number of eigenvalues with small magnitudes cannot be accounted to isolated clusters, as before. As an explanation, we suggest, that the eigenvectors of these eigenvalues are localized on a small subset of the graph's vertices. (This idea is supported by the high inverse participation ratios of these eigenvectors, see Fig.7).

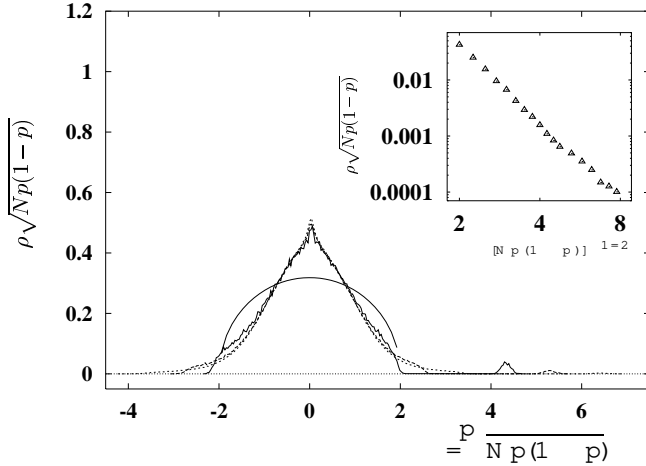


FIG. 4. Main panel: The average spectral densities of scale-free graphs with  $m = m_0 = 5$ , and  $N = 100$  (—),  $N = 300$  (---) and  $N = 1000$  (····) vertices. (In all three cases, the complete spectrum of 1000 graphs was used.) Another continuous line shows the semi-circular distribution for comparison. Observe that (i) the central part of the scale-free graph's spectral density is triangle-like, not semi-circular and (ii) the edges show a power-law decay, whereas the semi-circular distribution's edges decay exponentially, i.e., it decays exponentially at the edges [20]. In set: The upper edge of the spectral density for scale-free graphs with  $N = 20,000$  vertices the average degree of a vertex being  $\langle k_i \rangle = 2m = 10$ , as before. Note that both axes are logarithmic, indicating that ( ) has a power-law tail. Here, we used the iterative eigenvalue solver of Section III B 2 with  $n_d = 21$ ,  $n_{av} = 3$  and  $n_g = 60$  (for  $0 < 4.5 \frac{N p (1-p)}{p}$ ) and  $n_d = 2$ ,  $n_{av} = 27$  and  $n_g = 60$  (for  $0 > 4.5 \frac{N p (1-p)}{p}$ ).

1. The spectral density of the scale-free graph decays as a power-law

The inset of Fig.4 shows the tail of the bulk part of the spectral density for a graph with  $N = 20,000$  vertices and 100,000 edges (i.e.,  $\langle pN \rangle = 10$ ). Comparing this to the inset of Fig.1 ( where the number of vertices and edges is the same as here, ( one can observe the power-law decay at the edge of the bulk part of ( ). As shown later, in Section IV D, the power-law decay in this region is caused by eigenvectors localized on vertices with the highest degrees. The power-law decay of the degree sequence ( i.e., the existence of very high degrees ( is, in turn, due to the preferential attachment rule of the scale-free model.

2. The growth rate of the principal eigenvalue shows a crossover in the level of correlations

Since the adjacency matrix of a graph is a non-negative symmetric matrix, the graph's largest eigenvalue,  $\lambda_1$ , is also the largest in magnitude (see, e.g., Theorem 0.2 of Ref. [43]). Considering the effect of the adjacency matrix on the base vectors  $(\phi_i)_j = \delta_{ij}$  ( $i = 1; 2; \dots; N$ ), it can be shown that a lower bound for  $\lambda_1$  is given by the length of the longest row vector of the adjacency matrix, which is the square root of the graph's largest degree,  $k_1$ . Knowing that the largest degree of a scale-free graph grows as  $\sqrt{N}$  [1], one expects  $\lambda_1$  to grow as  $N^{1/4}$  for large enough systems.

Fig.5 shows a rescaled plot of the scale-free graph's largest eigenvalue for different values of  $m$ . In this figure,  $\lambda_1$  is compared to the length of the longest row vector,  $\sqrt{k_1}$  on the "natural scale" of these values, which is  $\frac{\lambda_1}{\sqrt{k_1}} \sim N^{1/4}$  [1]. It is clear that if  $m > 1$  and the system is small, then through several decades (a)  $\lambda_1$  is larger than  $\sqrt{k_1}$  and (b) the growth rate of  $\lambda_1$  is well below the expected rate of  $N^{1/4}$ . In the  $m = 1$  case, and for large systems, (a) the difference between  $\lambda_1$  and  $\sqrt{k_1}$  vanishes and (b) the growth rate of the principal eigenvalue will be maximal, too. This crossover in the behavior of the scale-free graph's principal eigenvalue is a specific property of sparse growing correlated graphs, and it is a result of the changing level of correlations between the longest row vectors (see Section V B).

3. Comparing the role of the principal eigenvalue in the scale-free graph and the  $m = 1$  uncorrelated random graph: a comparison of structures

Now we will compare the role of the principal eigenvalue in the  $m > 1$  scale-free graph and the  $m = 1$  uncorrelated random graph through its effect on the moments of the spectral density. On Figs.4 and 5, one can observe that (i) the principal eigenvalue of the scale-free graph

is detached from the rest of the spectrum, and (ii) as  $N \rightarrow \infty$ , it grows as  $N^{1-4}$  (see also Sections IV C 2 and V IB). It can be also seen, that in the limit, the bulk part will be symmetric, and its width will be constant (Fig. 4 rescales this constant width merely by another constant, namely  $N p[(1-p)]^{1-2}$ ). Because of the symmetry of the bulk part, in the  $N \rightarrow \infty$  limit, the third moment of  $\rho(\lambda)$  is determined exclusively by the contribution of the principal eigenvalue, which is  $N^{-1} \langle \lambda_1 \rangle^3 / N^{1-4}$ . For each moment above the third (e.g., for the  $l$ th moment), with growing  $N$ , the contribution of the bulk part to this moment will scale as  $O(1)$ , and the contribution of the principal eigenvalue will scale as  $N^{1+l-4}$ . In summary, in the  $N \rightarrow \infty$  limit, the scale-free graph's first eigenvalue has a significant contribution to the fourth moment; the 5th and all higher moments are determined exclusively by  $\lambda_1$ : the  $l$ th moment will scale as  $N^{1+l-4}$ .

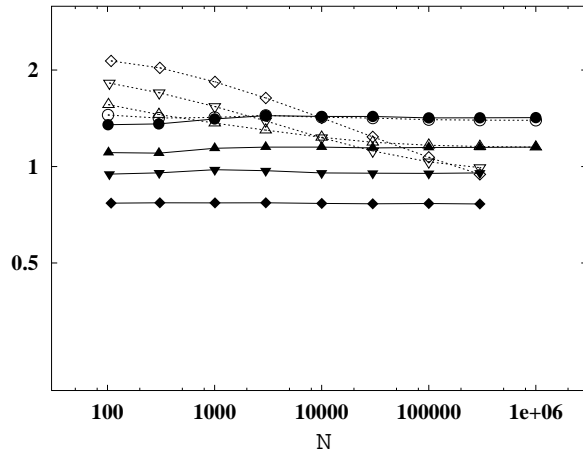


FIG. 5. Comparison of the length of the longest row vector,  $k_1$ , and the principal eigenvalue,  $\lambda_1$ , in scale-free graphs. Open symbols show  $\lambda_1 = (m N)^{1-4}$ , closed symbols show  $k_1 = (m N)^{1-4}$ . The parameter values are  $m = 1$  ( $\circ$ ),  $m = 2$  ( $\square$ ),  $m = 4$  ( $\triangle$ ) and  $m = 8$  ( $\diamond$ ). Each data point is an average for 9 graphs. For the reader's convenience, data points are connected.

If  $m > 1$  and the network is small, the principal eigenvalue,  $\lambda_1$ , of a scale-free graph is determined by the largest row vectors jointly: the largest eigenvalue is above  $k_1$  and the growth rate of  $\lambda_1$  stays below the maximum possible growth rate, which is  $\lambda_1 / N^{1-4}$ . If  $m = 1$ , or the network is large, the effect of row vectors other than the longest on  $\lambda_1$  vanishes: the principal eigenvalue converges to the length of the longest row vector, and it grows as  $\lambda_1 / N^{1-4}$ . Our results show a crossover in the growth rate of the scale-free model's principal eigenvalue.

In contrast to the above, the principal eigenvalue of the  $m = 1$  uncorrelated random graph converges to the constant  $pN = c$  in the  $N \rightarrow \infty$  limit, and the width of the bulk part also remains constant (see Fig. 2). Given a fixed number,  $l$ , the contribution of the principal eigenvalue to the  $l$ th moment of the spectral density will change as

$N^{-1} c^l$  in the  $N \rightarrow \infty$  limit. The contribution of the bulk part will scale as  $O(1)$ , therefore all even moments of the spectral density will scale as  $O(1)$  in the  $N \rightarrow \infty$  limit, and all odd moments will converge to 0.

The difference between the growth rate of the moments of  $\rho(\lambda)$  in the above two models (scale-free graph and  $m = 1$  uncorrelated random graph model) can be interpreted as a sign of different structure (see Section III A 1). In the  $N \rightarrow \infty$  limit, the average degree of a vertex converges to a constant in both models:  $\lim_{N \rightarrow \infty} \langle k_i \rangle = pN = c = 2m$ . (Both graphs will have the same number of edges per vertex.) On the other hand, in the limit, all moments of the  $m = 1$  uncorrelated random graph's spectral density converge to a constant, whereas the moments  $M_l(l = 5; 6; \dots)$  of the scale-free graph's  $\rho(\lambda)$  will diverge as  $N^{1+l-4}$ . In other words: the number of loops of length  $l$  in the  $m = 1$  uncorrelated random graph will grow as  $D_l = N M_l = O(N)$ , whereas for the scale-free graph for every  $l \geq 3$ , the number of these loops will grow as  $D_l = N M_l = O(N^{1-4})$ . From this we conclude that in the limit, the role of loops is negligible in the  $m = 1$  uncorrelated random graph, whereas it is large in the scale-free graph. In fact, the growth rate of the number of loops in the scale free graph exceeds all polynomial growth rates: the longer the loop size ( $l$ ) investigated, the higher the growth rate of the number of these loops ( $N^{1-4}$ ) will be. Note that the relative number of triangles (i.e., the third moment of the spectral density,  $M_3 = N^3$ ) will disappear in the scale-free graph, if  $N \rightarrow \infty$ .

In summary, the spectrum of the scale-free model converges to a triangle-like shape in the center, and the edges of the bulk part decay slowly. The first eigenvalue is detached from the rest of the spectrum, and it shows an anomalous growth rate. Eigenvalues with large magnitudes belong to eigenvectors localized on vertices with many neighbors. In the present context, the absence of triangles, the high number of loops with length above  $l = 3$ , and the buildup of correlations are the basic properties of the scale-free model.

#### D. Testing the structure of a "real-world" graph

To analyze the structure of a large sparse random graph (correlated or not), here we suggest several tests, that can be performed within  $O(N)$  CPU time, use  $O(N)$  floating point operations, and can clearly differentiate between the three "pure" types of random graph models treated in Section IV. Furthermore, these tests allow one to quantify the relation between any real-world graph and the three basic types of random graphs.

##### 1. Extremal eigenvalues

In Section III A 2 we have already mentioned that the extremal eigenvalues contain useful information on the

structure of the graph. As the spectra of uncorrelated random graphs (Fig.1) and scale-free networks (Fig.4) show, the principal eigenvalue of random graphs is often detached from the rest of the spectrum. For these two network types, the remaining bulk part of the spectrum { i.e., the set  $\{\lambda_2, \dots, \lambda_N\}$  } converges to a symmetric distribution, thus the quantity

$$R = \frac{\lambda_1 - \lambda_2}{\lambda_2 - \lambda_N} \quad (6)$$

measures the distance of the first eigenvalue from the main part of  $\{\lambda_i\}$  normalized by the extension of the main part.  $R$  can be connected to the chromatic number of the graph [52].

Note, that in the  $N \rightarrow \infty$  limit the  $\lambda_1 = 0$  sparse uncorrelated random graph's principal eigenvalue will scale as  $\langle k_i \rangle$ , whereas both  $\lambda_2$  and  $\lambda_N$  will scale as  $2 \sqrt{\langle k_i \rangle}$ . Therefore, if  $\langle k_i \rangle > 4$ , the principal eigenvalue will be detached from the bulk part of the spectrum and  $R$  will scale as  $(\langle k_i \rangle - 2)/4$ . If, however,  $\langle k_i \rangle \leq 4$ ,  $\lambda_1$  will not be detached from the bulk part, and it will converge to 0.

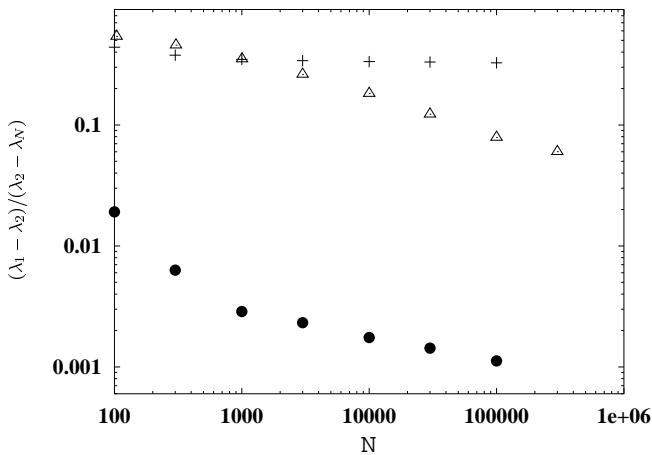


FIG. 6. The ratio  $R = (\lambda_1 - \lambda_2)/(\lambda_2 - \lambda_N)$  for sparse uncorrelated random graphs (+), small-world graphs with  $p_c = 0.01$  (x) and scale-free networks (4). All graphs have an average degree of  $\langle k_i \rangle = 10$ , and at each data point, the number of graphs used for averaging was 9. Observe, that for the uncorrelated random graph,  $R$  converges to a constant (see Section III A 2), whereas it decays rapidly for the two other types of networks, as  $N \rightarrow \infty$ . On the other hand, the latter two network types (small-world and scale-free) differ significantly in their magnitudes of  $R$ .

The above explanation and Fig.6 show that in the  $\langle k_i \rangle > 4$  sparse uncorrelated random graph model and the scale-free network,  $\lambda_1$  and the rest of the spectrum are well separated, which gives similarly high values for  $R$  in small systems. In large systems,  $R$  of the sparse uncorrelated random graph converges to a constant, while

$R$  in the scale-free model decays as a power law function of  $N$ . The reason for this drop is the increasing denominator on the rhs. of Eq.6:  $\lambda_2$  and  $\lambda_N$  are the extremal eigenvalues in the lower and upper long tails of  $\{\lambda_i\}$ , therefore, as  $N$  increases, the expectation values of  $\lambda_2$  and  $\lambda_N$  grow as quickly as that of  $\lambda_1$ . On the other hand, the small-world network shows much lower values of  $R$  already for small systems: here,  $\lambda_1$  is not detached from the rest of the spectrum, which is a consequence of the almost periodical structure of the graph.

On Fig.6, graphs with the same number of vertices and edges are compared. For large ( $N = 10;000$ ) systems, for sparse uncorrelated random graphs  $R$  converges to a constant, whereas for scale-free graphs and small-world networks it decays as a power-law. The latter two networks significantly differ in the magnitude of  $R$ . In summary, the suggested quantity  $R$  has been shown to be appropriate for distinguishing between the following graph structures: (i) periodical or almost periodical (small-world), (ii) uncorrelated non-periodical and (iii) strongly correlated non-periodical (scale-free).

## 2. Inverse participation ratios of extremal eigenpairs

Figure 7 shows the inverse participation ratios of the eigenvectors of an uncorrelated random graph, a small-world graph with  $p_c = 0.01$  and a scale-free graph. Even though all three graphs have the same number of vertices ( $N = 1;000$ ) and edges (5;000), one can observe rather specific features (see also the inset of Fig.7).

The uncorrelated random graph's eigenvectors show very little difference in their level of localization, except for the principal eigenvector, which is much less localized than the other eigenvectors;  $I(\lambda_2)$  and  $I(\lambda_N)$  are almost equal. For the small-world graph's eigenvectors,  $I(\lambda_i)$  has many different plateaus and spikes; the principal eigenvector is not localized, and the 2nd and  $N$ th eigenvectors have high, but different  $I(\lambda_i)$  values. The eigenvectors belonging to the scale-free graph's largest and smallest eigenvalues are localized on the "largest" vertices. The long tails of the bulk part of  $\{\lambda_i\}$  are due to these vertices. All three investigated eigenvectors ( $e_1, e_2$  and  $e_N$ ) of the scale-free graph are highly localized. Consequently, the inverse participation ratios of the eigenvectors  $e_1, e_2$  and  $e_N$  are handy for the identification of the 3 basic types of random graph models used.

## E. Structural variances

### 1. Relative variance of the principal eigenvalue for different types of networks: the scale-free graph and self-similarity

Figure 8 shows the relative variance of the principal eigenvalue { i.e.,  $(\lambda_1) = E(\lambda_1)$  } for the three basic random graph types.

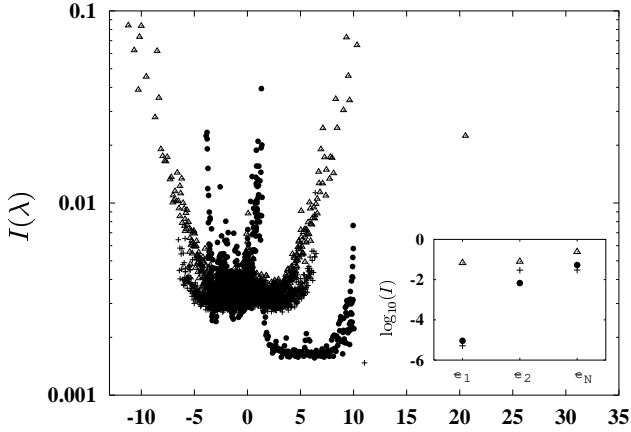


FIG. 7. Main panel: Inverse participation ratios of the eigenvectors of three graphs shown as a function of the corresponding eigenvalues: uncorrelated random graph (+), small-world graph with  $p_r = 0.01$  (•) and scale-free graph ( $\Delta$ ). All three graphs have  $N = 1;000$  vertices, and the average degree of a vertex is  $\langle k_i \rangle = 10$ . Observe, that the eigenvectors of the sparse uncorrelated random graph and the small-world network are usually non-localized ( $I(\lambda)$  is close to  $1/N$ ). On the contrary, eigenvectors belonging to the scale-free graph's extreme eigenvalues are highly localized with  $I(\lambda)$  approaching 0.1. Note also, that for  $\lambda = 0$ , the scale-free graph's  $I(\lambda)$  has a significant "spike" indicating again the localization of eigenvectors. Inset: Inverse participation ratios of the 1st, 2nd and  $N$ th eigenvectors of an uncorrelated random graph (+), a small-world graph with  $p_r = 0.01$  (•) and a scale-free graph ( $\Delta$ ). For each data point, the number of vertices was  $N = 300;000$  and the number of edges was  $1;500;000$ . Clearly, the principal eigenvector of the scale-free graph is localized, while the principal eigenvector of the other two systems (the uncorrelated models) is not. Note also, that the inverse participation ratios of the 2nd and  $N$ th eigenvectors clearly differ in the small-world graph (the spectrum of this graph has already been shown to be strongly asymmetric), whereas the inverse participation ratios of  $e_2$  and  $e_N$  are approximately the same in the uncorrelated random graph. Thus, with the help of the inverse participation ratios of  $e_1$ ,  $e_2$  and  $e_N$ , one can identify the three main types of random graphs used here.

For non-sparse uncorrelated random graphs ( $N \gg 1$  and  $p = \text{const}$ ) this quantity is known to decay at a rate which is faster than exponential [28,53]. Comparing sparse graphs with the same number of vertices and edges, one can see, that in the sparse uncorrelated random graph and the small-world model the relative variance of the principal eigenvalue drops quickly with growing system size. In the scale-free model, however, the relative variance of the principal eigenvalue's distribution remains constant with an increasing number of vertices.

In fractals, fluctuations do not disappear as the size of the system is increased, while in the scale-free graph, the relative variance of the principal eigenvalue is indepen-

dent of system size. In this sense, the scale-free graph resembles self-similar systems.

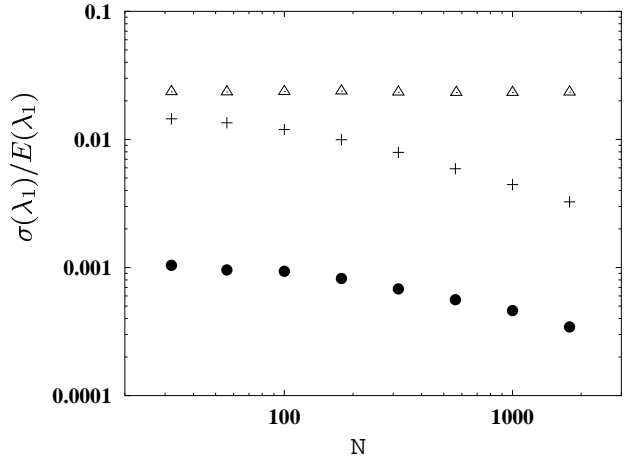


FIG. 8. Size dependence of the relative variance of the principal eigenvalue (i.e.,  $\sigma(\lambda_1)/E(\lambda_1)$ ) for sparse uncorrelated random graphs (+), small-world graphs with  $p_r = 0.01$  (•), and scale-free graphs ( $\Delta$ ). The average degree of a vertex is  $\langle k_i \rangle = 10$ , and 1000 graphs were used for averaging at every point. Observe, that in the uncorrelated random graph and the small-world model  $\sigma(\lambda_1)/E(\lambda_1)$  decays with increasing system size, however, for scale-free graphs with the same number of edges and vertices, it remains constant.

## V. CONCLUSIONS

We have performed a detailed analysis of the complete spectra, eigenvalues and the eigenvectors' inverse participation ratios in three types of sparse random graphs: the sparse uncorrelated random graph, the small-world model and the scale-free network. Connecting the topological features of these graphs to algebraic quantities, we have demonstrated that (i) the semi-circle law is not universal, not even for the uncorrelated random graph model; (ii) the small-world graph is inherently non-correlated and contains a high number of triangles; (iii) the spectral density of the scale-free graph is made up of three, well distinguishable parts (center, tails of bulk, first eigenvalue), and as  $N \gg 1$ , triangles become negligible and the level of correlations changes.

We have presented practical tools for the identification of the above mentioned basic types of random graphs and further, for the classification of real-world graphs. The robust eigenvector techniques and observations outlined in this paper combined with previous studies are likely to improve our understanding of large sparse correlated random structures. Examples for algebraic techniques already in use for large sparse correlated random structures are analyses of the Internet [6,18] and search engines [54] and mappings [55,56] of the World-Wide Web. Besides the improvement of these techniques, the present work

may turn out to be useful for analyzing the correlation structure of the transactions between a very high number of economical and financial units, which has already been started in e.g., Refs. [57-59]. Lastly, we hope to have provided quantitative tools for the classification of further "real-world" networks, e.g., social and biological networks.

## ACKNOWLEDGEMENTS

We thank D. Petz, G. Stoyan, G. Tusnady and K. Wu for helpful discussions. This research was partially supported by a HNSF Grant No. OTKA T 033104 and NSF PHY-9988674.

## VI. APPENDICES

A. The spectrum of a small-world graph for  $p_r = 0$  rewiring probability

### 1. Derivation of the spectral density

If the rewiring probability of a small-world graph is  $p_r = 0$ , then the graph is regular, each vertex is connected to its  $k$  nearest neighbors and the eigenvalues can be computed using the graph's symmetry operations. Rotational symmetry operations can be easily recognized, if the vertices of the graph are drawn along the perimeter of a circle (see Fig. 9): let  $P^{(n)}$  ( $n = 0; 1; \dots; N-1$ ) denote the symmetry operation that rotates the graph by  $n$  vertices in the anticlockwise direction. Being a symmetry operation, each  $P^{(n)}$  commutes with the adjacency matrix,  $A$ , and they have a common full orthogonal system of eigenvectors.

Now, we will create a full orthogonal basis of  $A$ . (We will treat only the case when  $N$  is an even number; odd  $N$ 's can be treated similarly.) It is known, that the eigenvalues of  $A$  are real, however, to simplify calculations, we will use complex numbers first. The eigenvectors of every  $P^{(n)}$  are  $e_1; e_2; \dots; e_N$ :

$$(e_1)_j = \exp \left[ 2i \frac{jl}{N} \right]; \quad (7)$$

where  $l = 0; 2; \dots; N-1$  and  $i = \sqrt{-1}$ . The eigenvalue of  $P^{(n)}$  on  $e_1$  is

$$s_1^{(n)} = \exp \left[ 2i \frac{nl}{N} \right]; \quad (8)$$

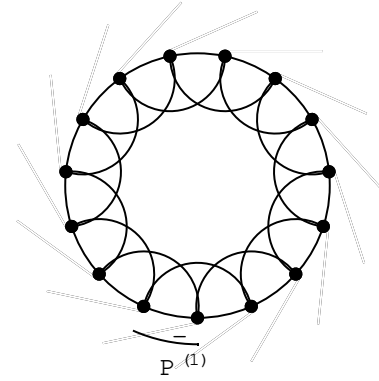


FIG. 9. The regular ring graph obtained from the small-world model in the  $p_r = 0$  case: rotations  $P^{(n)}$  for every  $n = 0; 1; \dots; N-1$  are symmetry operations of the graph. The  $P^{(n)}$  operators (there are  $N$  of them) can be used to create a full orthogonal basis of the adjacency matrix,  $A$ : taking any  $P^{(n)}$ , it commutes with  $A$ , therefore they have a common full orthogonal system of eigenvectors. (For a clear illustration of symmetries, this figure shows a graph with only  $N = 15$  vertices and  $k = 4$  connections per vertex.)

By adding these values pairwise, one can obtain the  $N$  eigenvalues of the graph:

$$\lambda_l = 2 \sum_{j=1}^{k/2} \cos \left[ 2 \frac{jl}{N} \right]; \quad (9)$$

In the previous exponential from the r.h.s. is a summation for a geometrical series, therefore

$$\lambda_l = \frac{\sin[(k+1)l/N]}{\sin(l/N)}; \quad (10)$$

In the  $N \rightarrow \infty$  limit, this converges to

$$\lambda(x) = \frac{\sin[(k+1)x]}{\sin(x)}; \quad (11)$$

where  $x$  is evenly distributed in the interval  $[0; \pi]$ .

### 2. Singularities of the spectral density

The spectral density is singular in  $\lambda = \lambda(x)$ , if and only if  $\frac{d}{dx} \lambda(x) = 0$ , which is equivalent to

$$(k+1) \tan(x) = \tan[(k+1)x]; \quad (12)$$

Since  $k$  is an even number, both this equation and Eq. (11) are invariant under the transformation  $x \rightarrow \pi - x$ , therefore only the  $x \in [0; \pi/2]$  solutions will give different values. If  $k = 10$  (see Fig. 3), Eq. (12) has  $k/2 + 1 = 6$  solutions in  $[0; \pi/2]$ , which are  $x = 0, 0.410, 0.704, 0.994, 1.28$  and  $\pi/2$ . Therefore (according to Eq. (11)) in the  $N \rightarrow \infty$  limit, the spectral density will be singular in the following points:

$$\lambda = 3.46; 2.19; 2; 0.043; 0.536; \text{ and } k = 10: \quad (13)$$

B. Crossover in the growth rate of the scale-free graph's principal eigenvalue

The largest eigenvalue is influenced only by the longest row vector if and only if the two longest row vectors are almost orthogonal:

$$v_1 \cdot v_2 = \sum_{j=1}^N v_{1j} v_{2j} \quad (14)$$

For  $m > 1$ , the lhs. of (14) is the number of simultaneous 1's in the two longest row vectors, and the rhs. can be approximated with  $\sum_{j=1}^N v_{1j} v_{2j} = k_1$ , the largest degree of the graph. It is known [11], that for large  $j$  ( $j > i$ ), the  $j$ th vertex will be connected to vertex  $i$  with probability  $P_{ij} = m = (2^{-i})^j$ . Thus, we can write (14) in the following form s:

$$\sum_{t=1}^N P_{1t}^2 = \sum_{t=1}^N P_{1t} m \quad (15)$$

or

$$\frac{P}{N_c} = \frac{m}{\ln N_c} \quad (16)$$

where  $N_c$  is the critical system size.

[1] P. Erdős and A. Rényi, "On random graphs," *Publicationes Mathematicae* 6 (1959) 290-297; P. Erdős and A. Rényi, "On the evolution of random graphs," *Publ. of the Math. Inst. of the Hung. Acad. of Sci.* 5 (1960) 17-61 (1959) 290-297; P. Erdős and A. Rényi, "On the strength of connectedness of a random graph," *Acta Math. Sci. Hung.* 12 (1961) 261-267

[2] B. Bollobas, *Random Graphs* (London, 1985)

[3] S. Redner, "How popular is your paper? An empirical study of the citation distribution," *Eur. Phys. J. B* 4 (1998) 131-134

[4] D. J. Watts and S. H. Strogatz, "Collective dynamics of 'small-world' networks," *Nature* 393 (1998) 440-442

[5] D. J. Watts, *Small Worlds: The Dynamics of Networks Between Order and Randomness* (Princeton Reviews in Complexity) (Princeton University Press, Princeton, New Jersey, 1999)

[6] M. Faloutsos, P. Faloutsos and C. Faloutsos, "On Power-Law Relationships of the Internet Topology," *ACM SIG-COMM '99; Comput. Commun. Rev.* 29 (1999) 251-263

[7] L. A. Adamic and B. A. Huberman, "Growth Dynamics of the World-Wide Web," *Nature* 401 (1999) 131

[8] R. Albert, H. Jeong and A.-L. Barabasi, "The diameter of the world wide web," *Nature* 401 (1999) 130-131

[9] H. Jeong, B. Tombor, R. Albert, Z. N. Oltvai and A.-L. Barabasi, "The large scale organization of metabolic networks," *Nature* 407 (2000) 651-654

[10] A.-L. Barabasi and R. Albert, "Emergence of scaling in random networks," *Science* 286 (1999) 509-512

[11] A.-L. Barabasi, R. Albert and H. Jeong, "Mean-field theory for scale-free random networks," *Physica A* 272 (1999) 173-187

[12] L. A. N. Amaral, A. Scala, M. Barthélemy, H. E. Stanley, "Classes of behavior of small-world networks," *cond-mat/0001458*

[13] A. L. Barabasi, H. Jeong, E. Ravasz, Z. Neda, T. Vicsek, A. Schubert, "Evolution of the scientific collaboration network," to be published.

[14] M. E. J. Newman, "The structure of scientific collaboration networks," *Proc. Natl. Acad. Sci. USA*, 98 (2001) 404-409; M. E. J. Newman, "Who is the best connected scientist? A study of scientific coauthorship networks," *cond-mat/0011144*

[15] Alberto Medina, Ibrahim Matta and John Byers, "On the Origin of Power Laws in Internet Topologies," *ACM SIG-COMM Computer Communication Review (CCR)* 30 (2) (2000) 18-28

[16] R. Cohen, K. Erez, D. ben-Avraham and S. Havlin, "Resilience of the Internet to random breakdowns," *Phys. Rev. Lett.* 85 (2000) 4626-4628

[17] R. Cohen, K. Erez, D. ben-Avraham, S. Havlin, "Breakdown of the Internet under intentional attack," *cond-mat/0010251*

[18] Broder, A., R. Kumar, F. M. Ghoul, P. Raghavan, S. Rajabopagan, R. Stata, A. Tomkins and J. Wiener, 2000, in *Proc. of the 9th Int. World-Wide Web Conf.*, <http://www.almaden.ibm.com/cs=k53/www9:na=i>.

[19] Petra M. Gleiss, Peter F. Stadler, Andreas Wagner and David A. Fell, "Small Cycles in Small Worlds," *Santa Fe Inst. Working Paper no. 00-10-058*

[20] M. L. Mehta. *Random Matrices*. 2nd ed. (Academic, New York, 1991)

[21] A. Crisanti, G. Paladin and A. Vulpiani, *Products of Random Matrices in Statistical Physics*, Springer Series in Solid-State Sciences 104 (Springer, Berlin, 1993)

[22] E. P. Wigner, "Characteristic Vectors of Bordered Matrices with Infinite Dimensions," *The Annals of Mathematics* 62 (1955) 548-564; E. P. Wigner, "Characteristic Vectors of Bordered Matrices with Infinite Dimensions II," *The Annals of Mathematics* 65 (1957) 203-207; E. P. Wigner, "On the Distribution of the Roots of Certain Symmetric Matrices," *The Annals of Mathematics* 67 (1958) 325-327

[23] F. Hiai and D. Petz. *The Semicircle Law, Free Random Variables and Entropy* (Am. Math. Soc., 2000) Section 4.1

[24] F. J. Dyson, "Statistical theory of the energy levels of complex systems I, II & III," *J. of Math. Phys.* 3 (1962) 140-175

[25] E. P. Wigner, "Random Matrices in Physics," *SIAM Review* 9 (1967) 1-23

[26] T. Guhr, A. Müller-Groeling and H. A. Weidenmüller "Random-matrix theories in quantum physics: common concepts," *Phys. Rep.* 299 (1998) 189-425

[27] F. Juhasz, "On the spectrum of a random graph," *Colloq. Math. Soc. Janos Bolyai* (1978) 313-316

[28] D. Cvetkovic, P. Rowlinson, "The Largest Eigenvalue of

- a Graph: A Survey," *Lin. and Multilin. Alg.* 28 (1990) 3-33
- [29] B. V. Bonch, "Accuracy of the Semicircle Approximation for the Density of Eigenvalues of Random Matrices," *J. Math. Phys.* 5, no. 2 (1964) 215-220
- [30] M. E. J. Newman, C. Moore, and D. J. Watts, "Mean-Field Solution of the Small-World Network Model," *Phys. Rev. Lett.* 84 (2000) 3201-3204
- [31] The number of edges meeting at one vertex of a graph is called the degree of that vertex, and a graph is called regular, if every vertex has the same degree.
- [32] P. L. Krapivsky and S. Redner, "Organization of Growing Random Networks," *cond-mat/0011094*
- [33] P. L. Krapivsky, G. J. Rodgers, and S. Redner, "Degree Distributions of Growing Networks," *cond-mat/0012181*
- [34] S. N. Dorogovtsev and J. F. F. Mendes, "Evolution of networks with aging of sites," *Phys. Rev. E* 62 (2000) 1842-1845
- [35] S. N. Dorogovtsev, J. F. F. Mendes and A. N. Samukhin, "Growing network with heritable connectivity of nodes," *cond-mat/0011077*
- [36] S. N. Dorogovtsev and J. F. F. Mendes, "Scaling properties of scale-free evolving networks: Continuous approach," *cond-mat/0012009*
- [37] R. Albert and A.-L. Barabasi, "Topology of evolving networks: local events and universality," *Phys. Rev. Lett.* 85 (2000) 5234-5237
- [38] G. Bianconi, A.-L. Barabasi, "Bose-Einstein condensation in complex networks," *cond-mat/0011224*
- [39] G. Bianconi, A.-L. Barabasi, "Competition and multi-scaling in evolving networks," *cond-mat/0011029*
- [40] A. Vazquez, "Knowing a network by walking on it: emergence of scaling," *cond-mat/0006132*
- [41] J. M. Montoya and R. V. Sole, "Small world patterns in food webs," *Santa Fe Inst. Working Paper no. 00-10-059*; R. V. Sole and J. M. Montoya, "Complexity and fragility in ecological networks," *Santa Fe Inst. Working Paper no. 00-10-060*
- [42] R. L. Graham, M. G. Rotschel, L. Lovasz, eds., *Handbook of Combinatorics* (North-Holland, Amsterdam, 1995).
- [43] D. M. Cvetkovic, M. Doob and H. Sachs, *Spectra of Graphs* (Berlin, 1980)
- [44] W. H. Press, S. A. Teukolsky, W. T. Vetterling and B. P. Flannery. *Numerical Recipes in C*, 2nd, reprinted ed. (Cambridge University Press, 1995) Sections 11.2 and 11.3
- [45] B. N. Parlett. *The symmetric eigenvalue problem*. SIAM, Philadelphia, PA, 1998.
- [46] K. Wu, A. Canning, H. D. Simon and L.-W. Wang: "Thick-restart Lanczos method for electronic structure calculations," *J. of Comp. Phys.* 154 (1999) 156-173
- [47] K. Wu and H. Simon, "Thick-restart Lanczos method for symmetric eigenvalue problems," Report No. 41412. Lawrence Berkeley National Laboratory. (1998)
- [48] B. Bollobas and A. G. Thomason, "Random graphs of small order," In *Random Graphs*, *Ann. of Discr. Math.*, 47-97 (1985)
- [49] If  $n_{s,e}$  denotes the number of isolated clusters with  $s$  vertices and  $e$  edges, then the number of isolated clusters of size  $s$  can be written as  $n_s = \sum_{e=s-1}^{s(s-1)/2} n_{s,e}$ .
- The  $e = s - 1$  case corresponds to stars of size  $s$ , and  $n_{s,s-1}$  can be given as  $\binom{N}{s} s^{s-1} (1-p)^{s(N-s)+\frac{s(s-1)}{2}}$ . If  $N \gg 1$  and  $pN \gg c$ , then for any finite  $s$  this converges to  $N f(s)$ , where  $f(s) = \binom{2}{s} s^{s-1} c^{s-1} \exp(-cs)$ , which is an exponentially decreasing function of  $s$ , if  $c > 1$ .
- Similarly to this case, in the  $N \gg 1$  and  $pN \gg c$  limit, for all values of  $e$ ,  $n_{s,e}$  is an exponentially decaying function of  $s$ , if  $c > 1$ . Since the number of possible  $e$  values for a fixed  $s$  is a polynomial function of  $s$ ,  $n_s$  will also decay exponentially, if  $c > 1$ ,  $N \gg 1$  and  $pN \gg c$ .
- [50] In a graph with  $N$  vertices, the contribution of one isolated vertex to the spectral density is  $N^{-1} \delta(\lambda)$ , and the contribution of an isolated cluster with two vertices is  $N^{-1} [(\lambda+1) + (\lambda-1)]$ . An isolated cluster with three vertices and two edges will give  $N^{-1} [(\lambda+\sqrt{2}) + (\lambda-\sqrt{2})]$ , and one with three vertices and three edges adds  $N^{-1} [2(\lambda+1) + (\lambda-2)]$  to the spectral density.
- [51] M. Barthelemy and L. A. N. Amaral, "Small-world networks: evidence for a crossover picture," *Phys. Rev. Lett.* 82 (1999) 3180-3183; erratum: *Phys. Rev. Lett.* 82 (1999) 5180
- [52] A graph is said to be properly colored, if any two vertices connected by an edge have different colors, and the chromatic number,  $\chi(G)$  of a graph  $G$  is the smallest such natural number,  $k$ , for which the graph can be properly colored using  $k$  colors. On a complete graph (a graph where any two vertices are connected) with  $N$  vertices,  $\chi = N$ , while on a tree,  $\chi = 2$ . It should be noted, that in general, the chromatic number of a graph is not determined by its spectrum; in fact, there exist graphs with identical spectra and different chromatic numbers [43]. A well-known relation [60] connecting the chromatic number and the extremal eigenvalues of any graph is the following:  $\chi(G) \leq 1 + \lambda_1 = \chi(N)$ .
- If the bulk part of the spectrum is symmetrical and the first eigenvalue is separated (as it is the case for uncorrelated random graphs and scale-free networks), then  $R$  can be written as  $(\lambda_1 - N) = (\lambda_2 - N) - 1 = 2 - 1$ .
- [53] C. M. Cidam, "On the method of bounded differences," *Surveys in Combinatorics*, 1989 (Norwich, 1989), 148-188 *London Math. Soc. Lecture Note Ser.*, 141 Cambridge Univ. Press, Cambridge, 1989.
- [54] J. Kleinberg, S. R. Kumar, P. Raghavan, S. Rajagopalan, and A. Tomkins, "The web as a graph: Measurements, models and methods," *Proc. of the Int. Conf. on Comb. and Comp.*, 1999; see also the homepage of the "CLEVER" project at <http://www.aladen.ibm.com/cs-k53=clever.htm>
- [55] The CAIDA Plankton project: Visualizing NLANR's Web Cache Hierarchy, <http://www.caida.org/tools/visualization/plankton.html>
- [56] Y. Shavit, X. Sun, A. W. W. and B. Yener, "Computing the Unmeasured: An Algebraic Approach to Internet Mapping", Lucent Technologies Technical Report 10009674-000214-01TM, February 2000.
- [57] L. Laloux, P. Cizeau, J.-P. Bouchaud, and M. Potters, "Noise Dressing of Financial Correlation Matrices," *Phys. Rev. Lett.* 83 (1999) 1467-1470
- [58] V. Perlerou, P. Gopikrishnan, B. Rosenow, L. A. N. Amaral

ral, and H. E. Stanley, "Universal and Nonuniversal Properties of Cross Correlations in Financial Time Series," Phys. Rev. Lett. 83 (1999) 1471-1474;  
[59] R. N. Mantegna, "Hierarchical Structure in Financial

Markets," cond-mat/9802256  
[60] N. Biggs. Algebraic Graph Theory. Cambridge University Press. (Cambridge, 1974)